



Asynchronous
filtering for
hydrological
forecasting

O. Rakovec et al.

This discussion paper is/has been under review for the journal Hydrology and Earth System Sciences (HESS). Please refer to the corresponding final paper in HESS if available.

Operational aspects of asynchronous filtering for hydrological forecasting

O. Rakovec^{1,3}, A. H. Weerts^{1,2}, J. Sumihar², and R. Uijlenhoet¹

¹Hydrology and Quantitative Water Management Group, Department of Environmental Sciences, Wageningen University, the Netherlands

²Deltares, P.O. Box 177, 2600 MH Delft, the Netherlands

³UFZ – Helmholtz Centre for Environmental Research, Leipzig, Germany

Received: 14 February 2015 – Accepted: 6 March 2015 – Published: 20 March 2015

Correspondence to: O. Rakovec (oldrich.rakovec@ufz.de)

Published by Copernicus Publications on behalf of the European Geosciences Union.

Title Page

Abstract

Introduction

Conclusions

References

Tables

Figures



Back

Close

Full Screen / Esc

Printer-friendly Version

Interactive Discussion



period, which incorporates the mismatch between the model and observations (e.g., Liu and Gupta, 2007).

A next distinction can be made between synchronous and asynchronous methods. Synchronous methods, also called three-dimensional (3-D), assimilate observations which correspond to the time of update. The Ensemble Kalman Filter (EnKF, e.g., Evensen, 2003) is a popular synchronous approach, which propagates an ensemble of model realizations over time and estimates the background error covariance matrix from the ensemble statistics. Asynchronous methods, also called four dimensional (4-D), refer to an updating methodology, in which observations being assimilated into the model originate from times different to the time of update (Evensen, 1994, 2009; Sakov et al., 2010). The Ensemble Kalman Smoother (EnKS) is a common example of an asynchronous method (e.g. Evensen and Van Leeuwen, 2000; Dunne and Entekhabi, 2006; Crow and Ryu, 2009; Li et al., 2013). The EnKS extends the EnKF by introducing additional information by propagating the contribution of future measurements backward in time. The EnKS reduces the error variance as compared to the EnKF for the past (Evensen, 2009). EnKS and EnKF are identical for forecasting (including nowcasting).

The essential difference between a smoother and a filter is that a smoother assimilates “future observations”, while a filter assimilates “past observations”. This implies that for operational forecasting purposes, we need a filter rather than a smoother. A smoother can help improve the model accuracy in the past (e.g. for re-analysis), but it does not help improve forecast accuracy (Evensen, 2009). Therefore, Sakov et al. (2010) introduced the Asynchronous Ensemble Kalman Filter (AEnKF), which requires forward integration of the model to obtain simulated results necessary for the analysis and model updating at the analysis step using past observations over a time window. The difference among the EnKF, EnKS and AEnKF is schematized in Fig. 1.

Sakov et al. (2010) showed that the formulation of the EnKS provides a method for asynchronous filtering, i.e. assimilating past data at once, and that the AEnKF is a generalization of the ensemble-based data assimilation technique. Moreover, unlike the

HESSD

12, 3169–3203, 2015

Asynchronous filtering for hydrological forecasting

O. Rakovec et al.

Title Page

Abstract

Introduction

Conclusions

References

Tables

Figures



Back

Close

Full Screen / Esc

Printer-friendly Version

Interactive Discussion



4-D variational assimilation methods, the AEnKF does not require any adjoint model (Sakov et al., 2010). The AEnKF is particularly attractive from an operational forecasting perspective as more observations can be used with hardly any extra additional computational time. Additionally, such an approach can potentially account for a better representation of the time-lag between the internal model states and the catchment response in terms of the discharge.

Discharge represents a widely used observation for assimilation into hydrological models, because it provides integrated catchment wetness estimates and is often available at high temporal resolution (Pauwels and De Lannoy, 2006; Teuling et al., 2010). Therefore, discharge is a popular variable in data assimilation studies used for model state updating (e.g., Weerts and El Serafy, 2006; Vrugt and Robinson, 2007; Blöschl et al., 2008; Clark et al., 2008; Komma et al., 2008; Pauwels and De Lannoy, 2009; Noh et al., 2011a; Pauwels et al., 2013) or dual state-parameter updating (e.g. Moradkhani et al., 2005b; Salamon and Feyen, 2009; Noh et al., 2011b).

The Kalman-type of assimilation methods was developed for an idealized modelling framework with perfect linear problems with Gaussian statistics, however, it has been demonstrated to work well for a large number of different nonlinear dynamical models (Evensen, 2009). It remains interesting to evaluate whether elimination of the non-linear nature from the model updating can be beneficial. For example, Xie and Zhang (2013) introduced the idea of a partitioned update scheme to reduce the degrees of freedom of the high-dimensional state-parameter estimation of a distributed hydrological model. In their study, the partitioned update scheme enabled to better capture covariances between states and parameters, which prevented spurious correlations of the non-linear relations in the catchment response. Similarly, decreasing the number of model states being perturbed and updated was suggested by McMillan et al. (2013) to increase the efficiency of the filtering algorithm while conserving the forecast quality. Such an approach was proposed especially to states with small innovations, which in their case was mainly the soil moisture storage.

**Asynchronous
filtering for
hydrological
forecasting**

O. Rakovec et al.

Title Page

Abstract

Introduction

Conclusions

References

Tables

Figures

◀

▶

◀

▶

Back

Close

Full Screen / Esc

Printer-friendly Version

Interactive Discussion



tion, quick flow and base flow. The latter two fluxes force the kinematic wave model (Chow et al., 1988; PCRaster, 2014). This routing scheme calculates the overland flow using two additional model states, the water level (H) and discharge (Q) accumulation over the drainage network. Model parameterization is based on the work of Booij (2002) and van Deursen (2004).

In contrast to Rakovec et al. (2012), in the current study we employed the HBV-96 model built within a recently developed open source modelling environment OpenStreams (2014), which is suitable for integrated hydrological modelling based on the Python programming language with the PCRaster spatial processing engine (Karssen-berg et al., 2009; PCRaster, 2014). The advantage of using OpenStreams (2014) is that it enables direct communication with OpenDA (2014), an open source data assimilation toolbox. OpenDA (2014) provides a number of algorithms for model calibration and assimilation and is suitable to be connected to any kind of environmental model (e.g., Ridler et al., 2014).

The import and export of hydrological and meteorological data to the system is done using Delft Flood Early Warning System (Delft-FEWS, Werner et al., 2013), an open shell system for managing forecasting processes and/or handling time series data. Delft-FEWS is a modular and highly configurable system, which is used by the Dutch authorities for the flood forecasting for the River Meuse basin (called RWsOS Rivers), in which the Upper Ourthe is located. The current configuration is a stand-alone version of RWsOS Rivers, however, it can be easily switched into a configuration with real-time data import.

2.2 Data assimilation for model initialization

As stated in the introduction, we investigate the potential added value of the Asynchronous EnKF (AEnKF) (Sakov et al., 2010) as compared to the traditional (synchronous) EnKF for operational flood forecasting. The derivation of the AEnKF (Sect. 2.2.2) is based on the equations using the same updating frequency (i.e., same

HESSD

12, 3169–3203, 2015

Asynchronous filtering for hydrological forecasting

O. Rakovec et al.

Title Page

Abstract

Introduction

Conclusions

References

Tables

Figures



Back

Close

Full Screen / Esc

Printer-friendly Version

Interactive Discussion



computational costs, different number of observations) for the EnKF (Sect. 2.2.1), as among others presented by Rakovec et al. (2012).

2.2.1 Ensemble Kalman Filter (EnKF)

First, we define a dynamic state space system as

$$5 \quad \mathbf{x}_k = f(\mathbf{x}_{k-1}, \boldsymbol{\theta}, \mathbf{u}_{k-1}) + \boldsymbol{\omega}_k, \quad (1)$$

where \mathbf{x}_k is a state vector at time k , f is an operator (hydrological model) expressing the model state transition from time step $k - 1$ to k in response to the model input \mathbf{u}_{k-1} and time-invariant model parameters $\boldsymbol{\theta}$. The noise term $\boldsymbol{\omega}_k$ is assumed to be Gaussian white noise (i.e., independent of time). It incorporates the overall uncertainties in model structure, parameters and model inputs.

Second, we define an observation process as

$$10 \quad \mathbf{y}_k = h(\mathbf{x}_k) + \mathbf{v}_k, \quad (2)$$

where \mathbf{y}_k is an observation vector derived from the model state \mathbf{x}_k and the model parameters through the h operator (in our case the kinematic wave model generating discharge). The noise term \mathbf{v}_k is additive observational Gaussian white noise, with zero mean and covariance \mathbf{R}_k . For independent measurement errors, \mathbf{R}_k is diagonal.

After the model update at time $k - 1$, the model is used to forecast model states at time k (Eq. 1). The grid-based model states form a matrix, which consists of N state vectors \mathbf{x}_k corresponding to N ensemble members:

$$20 \quad \mathbf{X}_k = (\mathbf{x}_k^1, \mathbf{x}_k^2, \dots, \mathbf{x}_k^N), \quad (3)$$

where

$$3175 \quad \mathbf{x}_k^i = (\text{SN}_{1:m}^i, \text{SM}_{1:m}^i, \text{UZ}_{1:m}^i, \text{LZ}_{1:m}^i, \text{H}_{1:m}^i, \text{Q}_{1:m}^i)^T, \quad (4)$$

Asynchronous filtering for hydrological forecasting

O. Rakovec et al.

Title Page

Abstract

Introduction

Conclusions

References

Tables

Figures

⏪

⏩

◀

▶

Back

Close

Full Screen / Esc

Printer-friendly Version

Interactive Discussion



SN^i , SM^i , UZ^i , LZ^i , H^i and Q^i are the HBV-96 model states of the i th ensemble member (Sect. 2.1), m gives the number of grid cells and T is the transpose operator. The ensemble mean

$$\bar{\mathbf{x}}_k = \frac{1}{N} \sum_{i=1}^N \mathbf{x}_k^i \quad (5)$$

is used to approximate the forecast error for each ensemble member:

$$\mathbf{E}_k = (\mathbf{x}_k^1 - \bar{\mathbf{x}}_k, \mathbf{x}_k^2 - \bar{\mathbf{x}}_k, \dots, \mathbf{x}_k^N - \bar{\mathbf{x}}_k). \quad (6)$$

The ensemble estimated model covariance matrix \mathbf{P}_k is defined as

$$\mathbf{P}_k = \frac{1}{N-1} \mathbf{E}_k \mathbf{E}_k^T. \quad (7)$$

When observations become available, the model states of i th ensemble member are updated as follows:

$$\mathbf{x}_k^{i,+} = \mathbf{x}_k^{i,-} + \mathbf{K}_k (\mathbf{y}_k - h(\mathbf{x}_k^{i,-}) + \mathbf{v}_k^i), \quad (8)$$

where $\mathbf{x}_k^{i,+}$ is the analysis (posterior, or update) model state matrix and $\mathbf{x}_k^{i,-}$ is the forecast (prior) model state matrix. \mathbf{K}_k is the Kalman gain, a weighting factor of the errors in model and observations:

$$\mathbf{K}_k = \mathbf{P}_k \mathbf{H}_k^T (\mathbf{H}_k \mathbf{P}_k \mathbf{H}_k^T + \mathbf{R}_k)^{-1}, \quad (9)$$

where $\mathbf{P}_k \mathbf{H}_k^T$ is approximated by the forecasted covariance between the model states and the forecasted discharge at the observing locations, and $\mathbf{H}_k \mathbf{P}_k \mathbf{H}_k^T$ is approximated

by the covariance of forecasted discharge at the observing locations (Houtekamer and Mitchell, 2001):

$$\mathbf{P}_k \mathbf{H}_k^T = \frac{1}{N-1} \sum_{i=1}^N (\mathbf{x}_k^i - \bar{\mathbf{x}}_k)(h(\mathbf{x}_k^i) - \overline{h(\mathbf{x}_k)})^T, \quad (10)$$

$$\mathbf{H}_k \mathbf{P}_k \mathbf{H}_k^T = \frac{1}{N-1} \sum_{i=1}^N (h(\mathbf{x}_k^i) - \overline{h(\mathbf{x}_k)})(h(\mathbf{x}_k^i) - \overline{h(\mathbf{x}_k)})^T, \quad (11)$$

where

$$\overline{h(\mathbf{x}_k)} = \frac{1}{N} \sum_{i=1}^N h(\mathbf{x}_k^i). \quad (12)$$

2.2.2 Asynchronous Ensemble Kalman Filter (AEnKF)

The AEnKF should not be considered as a new method, but rather a simple modification of the (synchronous) EnKF (Sect. 2.2.1) using a state augmentation approach. This means that the i th vector of model states (\mathbf{x}_k^i) at time k (see Eq. 4) is augmented with the past forecasted observations $h(\mathbf{x}_{k-1}^i), \dots, h(\mathbf{x}_{k-W}^i)$ (i.e., model outputs corresponding to the observation locations) from W previous time steps, which yields

$$\tilde{\mathbf{x}}_k^i = \begin{pmatrix} \mathbf{x}_k^i \\ h(\mathbf{x}_{k-1}^i) \\ h(\mathbf{x}_{k-2}^i) \\ \vdots \\ h(\mathbf{x}_{k-W}^i) \end{pmatrix}. \quad (13)$$

Remember that the size of \mathbf{x}_k^i and $h(\mathbf{x}_{k-1}^i), \dots, h(\mathbf{x}_{k-W}^i)$ can significantly differ: \mathbf{x}_k^i contains the complete set of model states, while $h(\mathbf{x}_{k-1}^i), \dots, h(\mathbf{x}_{k-W}^i)$ contains only the forecasted observations. Additionally, with the new state definition comes a new augmented observer operator $\tilde{\mathbf{h}}_k$ (in which I , with the corresponding subscript, stands for identity elements on the diagonal matching the dimensions in Eq. 13), a new augmented observation vector $\tilde{\mathbf{y}}_k$ and its corresponding observation covariance matrix $\tilde{\mathbf{R}}_k$:

$$\tilde{\mathbf{h}}_k = \begin{pmatrix} \mathbf{h}_k & & & & \\ & I_{k-1} & & & 0 \\ & & I_{k-2} & & \\ & 0 & & \ddots & \\ & & & & I_{k-W} \end{pmatrix}, \quad (14)$$

$$\tilde{\mathbf{y}}_k = \begin{pmatrix} \mathbf{y}_k \\ \mathbf{y}_{k-1} \\ \mathbf{y}_{k-2} \\ \vdots \\ \mathbf{y}_{k-W} \end{pmatrix}, \quad (15)$$

$$\tilde{\mathbf{R}}_k = \begin{pmatrix} \mathbf{R}_k & & & & \\ & \mathbf{R}_{k-1} & & & 0 \\ & & \mathbf{R}_{k-2} & & \\ & 0 & & \ddots & \\ & & & & \mathbf{R}_{k-W} \end{pmatrix}. \quad (16)$$

Having these augmented equations for $\tilde{\mathbf{x}}_k^i$, $\tilde{\mathbf{h}}_k$, $\tilde{\mathbf{y}}_k$ and $\tilde{\mathbf{R}}_k$, it is straightforward to carry out the assimilation in the same manner as presented in Sect. 2.2.1. Note that although current and past observations are used to construct the augmented state vector in the Eq. (13), in practice Eq. (8) is solved only to the current state $\tilde{\mathbf{x}}_k^i$ (i.e. the indices that

HESSD

12, 3169–3203, 2015

Asynchronous filtering for hydrological forecasting

O. Rakovec et al.

Title Page

Abstract

Introduction

Conclusions

References

Tables

Figures

◀

▶

◀

▶

Back

Close

Full Screen / Esc

Printer-friendly Version

Interactive Discussion



correspond to x_k^i) and the rest is ignored. The presence of past observation terms increases the dimension of $\tilde{\mathbf{P}}_k$ and $\tilde{\mathbf{K}}_k$ (see Eqs. 7 and 9) in both directions (rows and columns). Each column of $\tilde{\mathbf{K}}_k$ corresponds to an observation. The extra column of $\tilde{\mathbf{K}}_k$ corresponds to the past observations. Hence, it is possible to simply solve the equations for the first rows, which correspond only to x_k^i . Note that the first rows of $\tilde{\mathbf{K}}_k$ also contain the contributions of the past observations to the current state. These contributions arise from the off-diagonal terms of the augmented covariance $\tilde{\mathbf{P}}_k$. Finally, if the time window equals the current single time step, then $W = 0$ and the AEnKF problem reduces to the traditional EnKF.

From the operational point of view, it is preferable to have a longer assimilation window, because less frequent assimilation eliminates a disruption of the ensemble integration by an update and a restart. When assimilation is done more frequently, it will cause considerably higher calculation costs, which can often be a burden for real-time operational settings (Sakov et al., 2010). The AEnKF uses a longer assimilation window and assimilates all observations in a single update. This makes the AEnKF attractive to be used. The added value of a longer assimilation window will be a subject for investigation in this work. Especially, it can provide an improved representation of the time-lag between the internal model states and the catchment response in terms of the discharge. Such an idea was investigated for example by Li et al. (2013), who compared the effect of time-lag representation using the EnKF and EnKS.

2.3 Model uncertainty

In this study, we assume the source of model uncertainty to be the HBV soil moisture, which provides boundary conditions for surface runoff and represents interaction from interception, evapotranspiration, infiltration and input uncertainty by rainfall. The uncertainty is represented as a noise term ω as in Eq. (1). Based on expert knowledge, the noise is modelled as an autoregressive process of order 1 with a de-correlation time length of 4 h. The noise process is further assumed spatially isotropic with a spatial

Asynchronous filtering for hydrological forecasting

O. Rakovec et al.

Title Page

Abstract

Introduction

Conclusions

References

Tables

Figures



Back

Close

Full Screen / Esc

Printer-friendly Version

Interactive Discussion



Asynchronous filtering for hydrological forecasting

O. Rakovec et al.

Title Page

Abstract

Introduction

Conclusions

References

Tables

Figures



Back

Close

Full Screen / Esc

Printer-friendly Version

Interactive Discussion



The experimental setup scrutinizes the problem of asynchronous filtering from two perspectives. First, we investigate the effect of state augmentation using the past observations and assimilation of distributed observations on the state innovation (Sect. 3.1). Furthermore, the choice of which model states are included in the analysis step to be updated is analysed (Sects. 3.2, and 3.3). This means that besides updating all of the model states, we will test two other alternatives. The first alternative will leave out from the model analysis the soil moisture state (noSM), which is known to exhibit the most non-linear relation to Q. The second alternative will eliminate all the model states except for the two routing ones (HQ). The scenarios of the partitioned state updating schemes are shown in Table 2, including the control run without state updating (no update).

The performance of the data assimilation procedure regarding discharge forecasting is evaluated using the Ensemble Verification System (EVS): a software tool for verifying ensemble forecasts of hydrometeorological and hydrological variables at discrete locations (Brown et al., 2010), which provides a number of probabilistic verification measures. In this study we used three popular measures: the root mean square error (RMSE), the relative operating characteristic (ROC) score and the Brier skill (BS) score. We refer to e.g. Wilks (2006); Brown et al. (2010); Brown and Seo (2013), and Verkade et al. (2013) for exact definitions of these measures. In summary, the perfect forecast in terms of the RMSE has a value of 0, while positive values indicate errors in the same units as the variable. The perfect forecast in terms of the ROC and BS scores has a value of 1 and values smaller than 1 indicate forecast deterioration.

runs (top panel of Fig. 6) simulates the major flood peak reasonably well, including the timing and the magnitude. When discharge assimilation is employed, an overall reduction of the uncertainty in the forecasted ensemble is observed. Nevertheless, the forecasted flood peak becomes underestimated and the forecasted recession remains overestimated, which is acceptable because of the defined uncertainty in the observed discharge. This happens in particular for the scenario in which all states are updated; there are marginal differences between the non-augmented and augmented model states. Furthermore, when we leave out SM from the state update (noSM), we can observe that the major flood peak is forecasted more accurately, including the rising limb around 31 December 2002. Moreover, for the augmented state with $W = 11$, the ensemble spread becomes somewhat wider for lead times exceeding 12 h than for the non-augmented state. Nevertheless, the observations correspond approximately with the ensemble mean. Finally, we present the effect of the scenario in which only the two routing states are updated. The results suggest that the flood peak is captured most accurately of all scenarios, however with somewhat wider uncertainty bands. Therefore, it seems more appropriate to exclude the UZ storage (noSM scenario) in the model state updating, which represents water storage available for quick catchment response in the concept of the HBV model.

Besides a qualitative interpretation of the forecasted hydrographs presented in Fig. 6 for one particular event, we summarize these results in a more quantitative manner for the whole set of 8 flood events (see Table 1) in terms of the root-mean-square-error (RMSE) vs. lead time. This is shown in Fig. 7a for different partitioned state updating schemes and for three scenarios for the state augmentation at the catchment outlet (Tabreux). The control model run with no update has a constant RMSE of about $32 \text{ m}^3 \text{ s}^{-1}$ and an improved hydrological forecast has a RMSE lower than the control run. The results suggest that all assimilation scenarios improve the hydrological forecast, however with marked differences between the scenarios.

We can observe that updating all model states except for SM (noSM scenario) consistently leads to the most accurate forecasts across the whole range of lead times.

Asynchronous filtering for hydrological forecasting

O. Rakovec et al.

[Title Page](#)[Abstract](#)[Introduction](#)[Conclusions](#)[References](#)[Tables](#)[Figures](#)[Back](#)[Close](#)[Full Screen / Esc](#)[Printer-friendly Version](#)[Interactive Discussion](#)

Asynchronous filtering for hydrological forecasting

O. Rakovec et al.

Title Page

Abstract

Introduction

Conclusions

References

Tables

Figures



Back

Close

Full Screen / Esc

Printer-friendly Version

Interactive Discussion



Additionally, state augmentation using $W = 5$ and $W = 11$ indicates improvements compared to the case without augmentation ($W = 0$). However, for lead times longer than the travel time from the most upstream gauges to the outlet (i.e. exceeding 20 h), the difference between state augmentations $W = 5$ and $W = 11$ diminishes. Moreover, when only the two routing states (HQ scenario) are updated, the RMSE is lowered for short lead times, but the improved effect does not last as long as for the noSM scenario. The smallest improvement at shorter lead times is achieved when all model states are updated (scenario all). This is due to the strongly non-linear relation between the assimilated observations and the SM storage, which is further articulated by the time-lag between the state and the catchment response. Nevertheless, for longer lead times it seems slightly better to update all states rather than only the routing states.

Validation of the model setup in terms of the RMSE is presented in Fig. 7d for an independent evaluation of the forecasting results at Durbuy, an interior location, which was not used for assimilation. These results show that an improvement of discharge assimilation also occurs at the validation location and that the pattern corresponds well to the results presented in Fig. 7a. Such an analysis indicates that there is no spurious update of the model states.

To present the results in a more robust way, we also analyzed them (at Tabreux) in terms of other probabilistic verification measures: the relative operating characteristic (ROC) score and the Brier skill (BS) score (see Fig. 7b, c). Recall that values of 1 represent a perfect forecast, while values smaller than 1 indicate forecast deterioration. Similar to the RMSE results, updating only the two routing states (HQ) is most efficient for short lead times, but this skill disappears quickly for longer lead times. In terms of the ROC and BS scores, for a given augmentation size, there are marginal differences between the scenarios which update all states (all) and which leave the soil moisture out (noSM). However, it is notable that the state augmentation case ($W = 11$) improves the forecast performance as compared to the no augmentation case ($W = 0$). Note that the state augmentation of $W = 5$ was not carried out.

3.3 Temporal nature of model state innovations

To reveal the temporal nature of the model being updated using the AEnKF, using $W = 0$ and $W = 11$, we present in Fig. 8a and b time series of normalized differences between the ensemble means for the 3 partitioned update schemes and the ensemble mean for the no update scenario. The normalization is achieved by dividing the aforementioned difference by the no update scenario mean. In such a way we obtain the relative change in each of the model states. For the AEnKF using $W = 0$ (Fig. 8a), we can observe that for the scenario “all”, which updates all the model states, the magnitude of the percentage change is approximately the same for all 4 model states and ranges up to 25%. When all model states except for the SM are updated, no changes in the SM storage occur and the overall magnitude of the changes in the other states is slightly decreased and smoothed. Furthermore, when only the two routing states are updated (HQ), the SM and UZ storages remain constant over time and we observe a different temporal behaviour of the routing states in comparison with the previous cases. For the HQ scenario, the updated time series have a clear zigzag shape, which indicates that the effect of updating diminishes faster, because only the river channel is updated. In contrast, the routing states for the other cases show a more stable behaviour over time, illustrated by the stepwise shape. These more persistent results correspond to the updates in the UZ storage, which is used for a quick catchment response and has an impact for a longer time. The benefits of including the UZ storage in the update and leaving the SM storage out was already presented from a different point of view in Fig. 7a for longer lead times.

For the AEnKF using $W = 11$ (Fig. 8b), we can observe that the overall pattern of the temporal changes in the model states is similar as for $W = 0$, but the behaviour of using $W = 11$ shows somewhat larger variability. By assimilating more observations ($W = 11$), we expect even a larger update, assuming that more observations contain more information about the unknown truth. Assuming the underlying forecast model

HESSD

12, 3169–3203, 2015

Asynchronous filtering for hydrological forecasting

O. Rakovec et al.

Title Page

Abstract

Introduction

Conclusions

References

Tables

Figures

⏪

⏩

◀

▶

Back

Close

Full Screen / Esc

Printer-friendly Version

Interactive Discussion



Asynchronous filtering for hydrological forecasting

O. Rakovec et al.

Title Page

Abstract

Introduction

Conclusions

References

Tables

Figures

⏪

⏩

◀

▶

Back

Close

Full Screen / Esc

Printer-friendly Version

Interactive Discussion



Brown, J. D. and Seo, D.-J.: Evaluation of a nonparametric post-processor for bias correction and uncertainty estimation of hydrologic predictions, *Hydrol. Process.*, 27, 83–105, doi:10.1002/hyp.9263, 2013. 3181

5 Brown, J. D., Demargne, J., Seo, D.-J., and Liu, Y.: The Ensemble Verification System (EVS): a software tool for verifying ensemble forecasts of hydrometeorological and hydrologic variables at discrete locations, *Environ. Modell. Softw.*, 25, 854–872, doi:10.1016/j.envsoft.2010.01.009, 2010. 3181

Chow, V. T., Maidment, D., and Mays, L.: *Applied Hydrology*, McGraw-Hill, New York, USA, 1988. 3174

10 Clark, M. P., Rupp, D. E., Woods, R. A., Zheng, X., Ibbitt, R. P., Slater, A. G., Schmidt, J., and Uddstrom, M. J.: Hydrological data assimilation with the ensemble Kalman filter: use of streamflow observations to update states in a distributed hydrological model, *Adv. Water Resour.*, 31, 1309–1324, doi:10.1016/j.advwatres.2008.06.005, 2008. 3172, 3180

15 Crow, W. T. and Ryu, D.: A new data assimilation approach for improving runoff prediction using remotely-sensed soil moisture retrievals, *Hydrol. Earth Syst. Sci.*, 13, 1–16, doi:10.5194/hess-13-1-2009, 2009. 3171

20 Driessen, T. L. A., Hurkmans, R. T. W. L., Terink, W., Hazenberg, P., Torfs, P. J. J. F., and Uijlenhoet, R.: The hydrological response of the Ourthe catchment to climate change as modelled by the HBV model, *Hydrol. Earth Syst. Sci.*, 14, 651–665, doi:10.5194/hess-14-651-2010, 2010. 3173

Dunne, S. and Entekhabi, D.: Land surface state and flux estimation using the ensemble Kalman smoother during the Southern Great Plains 1997 field experiment, *Water Resour. Res.*, 42, 1–15, doi:10.1029/2005WR004334, 2006. 3171

25 Evensen, G.: Sequential data assimilation with a nonlinear quasi-geostrophic model using Monte Carlo methods to forecast error statistics, *J. Geophys. Res.*, 99, 10143–10162, 1994. 3170, 3171

Evensen, G.: The Ensemble Kalman Filter: theoretical formulation and practical implementation, *Ocean Dynam.*, 53, 343–367, 2003. 3171

30 Evensen, G.: *Data Assimilation: the Ensemble Kalman Filter*, Springer, Berlin, Heidelberg, Germany, 2009. 3170, 3171, 3172, 3196

Evensen, G. and Van Leeuwen, P.: An ensemble Kalman smoother for nonlinear dynamics, *Mon. Weather Rev.*, 128, 1852–1867, 2000. 3171

Asynchronous filtering for hydrological forecasting

O. Rakovec et al.

[Title Page](#)

[Abstract](#)

[Introduction](#)

[Conclusions](#)

[References](#)

[Tables](#)

[Figures](#)

[⏪](#)

[⏩](#)

[◀](#)

[▶](#)

[Back](#)

[Close](#)

[Full Screen / Esc](#)

[Printer-friendly Version](#)

[Interactive Discussion](#)



- Hazenberg, P., Leijnse, H., and Uijlenhoet, R.: Radar rainfall estimation of stratiform winter precipitation in the Belgian Ardennes, *Water Resour. Res.*, 47, 1–15, doi:10.1029/2010WR009068, 2011. 3183
- Houtekamer, P. L. and Mitchell, H. L.: A sequential ensemble Kalman filter for atmospheric data assimilation, *Mon. Weather Rev.*, 129, 123–137, 2001. 3177
- Karszenberg, D., Schmitz, O., Salamon, P., De Jong, C., and Bierkens, M. F. P.: A software framework for construction of process-based stochastic spatio-temporal models and data assimilation, *Environ. Modell. Softw.*, 25, 1–14, doi:10.1016/j.envsoft.2009.10.004, 2009. 3174
- Komma, J., Blöschl, G., and Reszler, C.: Soil moisture updating by ensemble Kalman filtering in real-time flood forecasting, *J. Hydrol.*, 357, 228–242, doi:10.1016/j.jhydrol.2008.05.020, 2008. 3172
- Lee, H., Seo, D.-J., and Koren, V.: Assimilation of streamflow and in situ soil moisture data into operational distributed hydrologic models: effects of uncertainties in the data and initial model soil moisture states, *Adv. Water Resour.*, 34, 1597–1615, doi:10.1016/j.advwatres.2011.08.012, 2011. 3188
- Li, Y., Ryu, D., Western, A. W., and Wang, Q. J.: Assimilation of stream discharge for flood forecasting: the benefits of accounting for routing time lags, *Water Resour. Res.*, 49, 1887–1900, doi:10.1002/wrcr.20169, 2013. 3171, 3179
- Lindström, G., Johansson, B., Persson, M., Gardelin, M., and Bergström, S.: Development and test of the distributed HBV-96 hydrological model, *J. Hydrol.*, 201, 272–288, 1997. 3173
- Liu, Y. and Gupta, H. V.: Uncertainty in hydrologic modeling: toward an integrated data assimilation framework, *Water Resour. Res.*, 43, 1–19, doi:10.1029/2006WR005756, 2007. 3170, 3171
- Liu, Y., Weerts, A. H., Clark, M., Hendricks Franssen, H.-J., Kumar, S., Moradkhani, H., Seo, D.-J., Schwanenberg, D., Smith, P., van Dijk, A. I. J. M., van Velzen, N., He, M., Lee, H., Noh, S. J., Rakovec, O., and Restrepo, P.: Advancing data assimilation in operational hydrologic forecasting: progresses, challenges, and emerging opportunities, *Hydrol. Earth Syst. Sci.*, 16, 3863–3887, doi:10.5194/hess-16-3863-2012, 2012. 3170
- McMillan, H. K., Hreinsson, E. Ö., Clark, M. P., Singh, S. K., Zammit, C., and Uddstrom, M. J.: Operational hydrological data assimilation with the recursive ensemble Kalman filter, *Hydrol. Earth Syst. Sci.*, 17, 21–38, doi:10.5194/hess-17-21-2013, 2013. 3172
- Moore, R. J.: The PDM rainfall-runoff model, *Hydrol. Earth Syst. Sci.*, 11, 483–499, doi:10.5194/hess-11-483-2007, 2007. 3187

Asynchronous filtering for hydrological forecasting

O. Rakovec et al.

Title Page

Abstract

Introduction

Conclusions

References

Tables

Figures

⏪

⏩

◀

▶

Back

Close

Full Screen / Esc

Printer-friendly Version

Interactive Discussion



- Moradkhani, H., Hsu, K. L., Gupta, H., and Sorooshian, S.: Uncertainty assessment of hydrologic model states and parameters: sequential data assimilation using the particle filter, *Water Resour. Res.*, 41, 1–17, 2005a. 3170
- Moradkhani, H., Sorooshian, S., Gupta, H., and Houser, P. R.: Dual state-parameter estimation of hydrological models using ensemble Kalman filter, *Adv. Water Resour.*, 28, 135–147, 2005b. 3170, 3172
- Noh, S. J., Tachikawa, Y., Shiiba, M., and Kim, S.: Applying sequential Monte Carlo methods into a distributed hydrologic model: lagged particle filtering approach with regularization, *Hydrol. Earth Syst. Sci.*, 15, 3237–3251, doi:10.5194/hess-15-3237-2011, 2011. 3172
- Noh, S. J., Tachikawa, Y., Shiiba, M., and Kim, S.: Dual state-parameter updating scheme on a conceptual hydrologic model using sequential Monte Carlo filters, *J. Jpn. Soc. Civil Engin. B1*, 67, I1–I6, 2011b. 3172
- Noh, S. J., Rakovec, O., Weerts, A. H., and Tachikawa, Y.: On noise specification in data assimilation schemes for improved flood forecasting using distributed hydrological models, *J. Hydrol.*, 519, 2707–2721, doi:10.1016/j.jhydrol.2014.07.049, 2014. 3180
- OpenDA: The OpenDA data-assimilation toolbox, available at: <http://www.opendata.org>, (last access: 1 November 2014), 2014. 3174, 3180
- OpenStreams: OpenStreams, available at: www.openstreams.nl, (last access: 1 November 2014), 2014. 3174
- Pauwels, V. R. N. and De Lannoy, G. J. M.: Improvement of modeled soil wetness conditions and turbulent fluxes through the assimilation of observed discharge, *J. Hydrometeorol.*, 7, 458–477, doi:10.1175/JHM490.1, 2006. 3172
- Pauwels, V. R. N., and De Lannoy, G. J. M.: Ensemble-based assimilation of discharge into rainfall–runoff models: a comparison of approaches to mapping observational information to state space, *Water Resour. Res.*, 45, 1–17, doi:10.1029/2008WR007590, 2009. 3172
- Pauwels, V. R. N., De Lannoy, G. J. M., Hendricks Franssen, H.-J., and Vereecken, H.: Simultaneous estimation of model state variables and observation and forecast biases using a two-stage hybrid Kalman filter, *Hydrol. Earth Syst. Sci.*, 17, 3499–3521, doi:10.5194/hess-17-3499-2013, 2013. 3172
- PCRaster: PCRaster Environmental Modelling language, available at: <http://pcraster.geo.uu.nl>, (last access: 1 November 2014), 2014. 3174
- Rafieeinassab, A., Seo, D.-J., Lee, H., and Kim, S.: Comparative evaluation of Maximum Likelihood Ensemble Filter and Ensemble Kalman Filter for real-time assimila-

Asynchronous filtering for hydrological forecasting

O. Rakovec et al.

[Title Page](#)

[Abstract](#)

[Introduction](#)

[Conclusions](#)

[References](#)

[Tables](#)

[Figures](#)

[⏪](#)

[⏩](#)

[◀](#)

[▶](#)

[Back](#)

[Close](#)

[Full Screen / Esc](#)

[Printer-friendly Version](#)

[Interactive Discussion](#)



tion of streamflow data into operational hydrologic models, *J. Hydrol.*, 519, 2663–2675, doi:10.1016/j.jhydrol.2014.06.052, 2014. 3188

Rakovec, O., Weerts, A. H., Hazenberg, P., Torfs, P. J. J. F., and Uijlenhoet, R.: State updating of a distributed hydrological model with Ensemble Kalman Filtering: effects of updating frequency and observation network density on forecast accuracy, *Hydrol. Earth Syst. Sci.*, 16, 3435–3449, doi:10.5194/hess-16-3435-2012, 2012. 3173, 3174, 3175, 3180, 3197, 3198

Reichle, R. H.: Data assimilation methods in the Earth sciences, *Water Resour.*, 31, 1411–1418, doi:10.1016/j.advwatres.2008.01.001, 2008. 3170

Ridler, M. E., van Velzen, N., Hummel, S., Sandholt, I., Falk, A. K., Heemink, A., and Madson, H.: Data assimilation framework: linking an open data assimilation library (OpenDA) to a widely adopted model interface (OpenMI), *Environ. Modell. Softw.*, 57, 76–89, doi:10.1016/j.envsoft.2014.02.008, 2014. 3174

Sakov, P., Evensen, G., and Bertino, L.: Asynchronous data assimilation with the EnKF, *Tellus A*, 62, 24–29, doi:10.1111/j.1600-0870.2009.00417.x, 2010. 3171, 3172, 3174, 3179, 3187

Salamon, P. and Feyen, L.: Assessing parameter, precipitation, and predictive uncertainty in a distributed hydrological model using sequential data assimilation with the particle filter, *J. Hydrol.*, 376, 428–442, 2009. 3172

Teuling, A., Lehner, I., Kirchner, J., and Seneviratne, S.: Catchments as simple dynamical systems: experience from a Swiss prealpine catchment, *Water Resour. Res.*, 46, 1–15, doi:10.1029/2009WR008777, 2010. 3172

van Deursen, W.: Afregelen HBV model Maasstroomgebied, Tech. rep., Rapportage aan RIZA. Carthago Consultancy, Rotterdam, the Netherlands, 2004. 3174

Verkade, J. S., Brown, J. D., Reggiani, P., and Weerts, A. H.: Post-processing ECMWF precipitation and temperature ensemble reforecasts for operational hydrologic forecasting at various spatial scales, *J. Hydrol.*, 501, 73–91, doi:10.1016/j.jhydrol.2013.07.039, 2013. 3181

Vrugt, J. A. and Robinson, B. A.: Treatment of uncertainty using ensemble methods: comparison of sequential data assimilation and Bayesian model averaging, *Water Resour. Res.*, 43, 1–15, doi:10.1029/2005WR004838, 2007. 3172

Wanders, N., Bierkens, M. F. P., de Jong, S. M., de Roo, A., and Karszenberg, D.: The benefits of using remotely sensed soil moisture in parameter identification of large-scale hydrological models, *Water Resour. Res.*, 50, 6874–6891, doi:10.1002/2013WR014639, 2014a. 3188

**Asynchronous
filtering for
hydrological
forecasting**

O. Rakovec et al.

[Title Page](#)[Abstract](#)[Introduction](#)[Conclusions](#)[References](#)[Tables](#)[Figures](#)[⏪](#)[⏩](#)[◀](#)[▶](#)[Back](#)[Close](#)[Full Screen / Esc](#)[Printer-friendly Version](#)[Interactive Discussion](#)

- Wanders, N., Karssenbergh, D., de Roo, A., de Jong, S. M., and Bierkens, M. F. P.: The suitability of remotely sensed soil moisture for improving operational flood forecasting, *Hydrol. Earth Syst. Sci.*, 18, 2343–2357, doi:10.5194/hess-18-2343-2014, 2014b. 3188
- 5 Weerts, A. H. and El Serafy, G. Y. H.: Particle filtering and ensemble Kalman filtering for state updating with hydrological conceptual rainfall–runoff models, *Water Resour. Res.*, 42, 1–17, doi:10.1029/2005WR004093, 2006. 3170, 3172, 3180
- Werner, M., Schellekens, J., Gijsbers, P., van Dijk, M., van den Akker, O., and Heynert, K.: The Delft-FEWS flow forecasting system, *Environ. Modell. Softw.*, 40, 65–77, doi:10.1016/j.envsoft.2012.07.010, 2013. 3174
- 10 Wilks, D. S.: *Statistical Methods in the Atmospheric Sciences*, Elsevier, San Diego, 2006. 3181
- Xie, X. and Zhang, D.: A partitioned update scheme for state-parameter estimation of distributed hydrologic models based on the ensemble Kalman filter, *Water Resour. Res.*, 49, 7350–7365, doi:10.1002/2012WR012853, 2013. 3172, 3187
- 15 Zhou, Y., McLaughlin, D., and Entekhabi, D.: Assessing the performance of the ensemble Kalman filter for land surface data assimilation, *Mon. Weather Rev.*, 134, 2128–2142, 2006. 3170
- Zupanski, M.: Maximum Likelihood Ensemble Filter: theoretical aspects, *Mon. Weather Rev.*, 133, 1710–1726, doi:10.1175/MWR2946.1, 2005. 3188

**Asynchronous
filtering for
hydrological
forecasting**

O. Rakovec et al.

[Title Page](#)[Abstract](#)[Introduction](#)[Conclusions](#)[References](#)[Tables](#)[Figures](#)[Back](#)[Close](#)[Full Screen / Esc](#)[Printer-friendly Version](#)[Interactive Discussion](#)**Table 1.** Overview of the periods used in this study.

Period	Number of events	Maximum observed discharge [$\text{m}^3 \text{s}^{-1}$]
23 Oct 1998–15 Nov 1998	1	210
15 Feb 1999–5 Mar 1999	2	195
15 Jan 2002–6 Mar 2002	4	340
21 Dec 2002–7 Jan 2003	1	380

HESSD

12, 3169–3203, 2015

Asynchronous filtering for hydrological forecasting

O. Rakovec et al.

Table 2. Four partitioned state updating schemes (indicated in the first column) for 5 model states (indicated in the first row) being updated and thus included in the model analysis. Model states are described in Sect. 2.1 and Fig. 3 and have following acronyms: discharge (Q), water level (H), soil moisture storage (SM), snow storage (SN), upper zone storage (UZ), and lower zone storage (LZ).

Name	Q	H	SM	SN	UZ	LZ
No update						
all	✓	✓	✓	✓	✓	✓
noSM	✓	✓		✓	✓	✓
HQ	✓	✓				

Title Page

Abstract Introduction

Conclusions References

Tables Figures

⏪ ⏩

◀ ▶

Back Close

Full Screen / Esc

Printer-friendly Version

Interactive Discussion



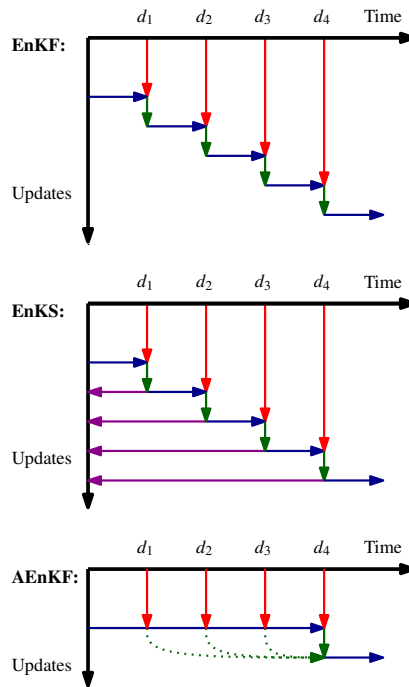


Figure 1. Illustration of the model updating procedure for the Ensemble Kalman Filter (EnKF), the Ensemble Kalman Smoother (EnKS), and the Asynchronous Ensemble Kalman Filter (AEnKF). The horizontal axis stands for time, observations (d_1 , d_2 , d_3 , d_4) are given at regular intervals. The blue arrows represent forward model integration, the red arrows denote introduction of observations and green arrows indicate model update. The magenta arrows represent the model updates for the EnKS, therefore they go backward in time, as they are computed following the EnKF update every time observations become available. The green dotted arrows denote past observations being assimilated using the AEnKF. The schemes for the EnKF and the EnKS are after Evensen (2009).

Asynchronous filtering for hydrological forecasting

O. Rakovec et al.

Title Page	
Abstract	Introduction
Conclusions	References
Tables	Figures
◀	▶
◀	▶
Back	Close
Full Screen / Esc	
Printer-friendly Version	
Interactive Discussion	



Asynchronous filtering for hydrological forecasting

O. Rakovec et al.

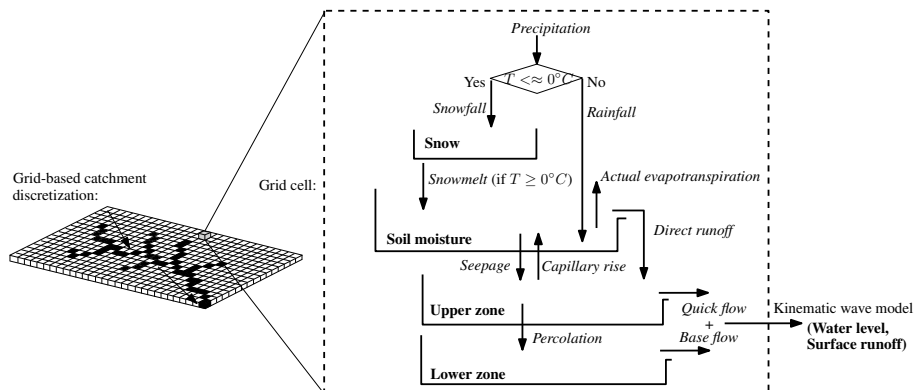


Figure 3. Left: catchment discretization using a grid-based approach including the channel delineation. Arrows indicate flow direction. Right: schematic structure of the HBV-96 model for each grid cell. Model states are in bold and model fluxes in italics (after Rakovec et al., 2012).

Title Page

Abstract

Introduction

Conclusions

References

Tables

Figures

◀

▶

◀

▶

Back

Close

Full Screen / Esc

Printer-friendly Version

Interactive Discussion

Asynchronous filtering for hydrological forecasting

O. Rakovec et al.

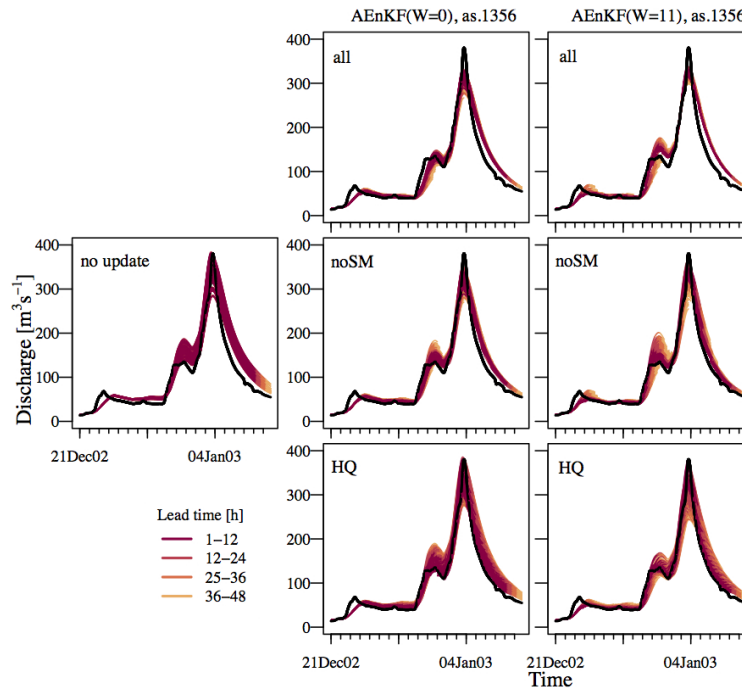


Figure 6. Ensemble of discharge forecasts for a typical event at the catchment outlet (Tabreux, gauge 1) for different updating scenarios. The control run (with no update) is shown in the top panel. The combined effect of the model states being updated (3 scenarios shown in rows) and the length of the state augmentation vector (W) of past observations being assimilated (2 scenarios in columns) is presented. The observations are shown in black. Gauges 1, 3, 5, and 6 are assimilated.

[Title Page](#)
[Abstract](#)
[Introduction](#)
[Conclusions](#)
[References](#)
[Tables](#)
[Figures](#)
[⏪](#)
[⏩](#)
[◀](#)
[▶](#)
[Back](#)
[Close](#)
[Full Screen / Esc](#)
[Printer-friendly Version](#)
[Interactive Discussion](#)

Asynchronous filtering for hydrological forecasting

O. Rakovec et al.

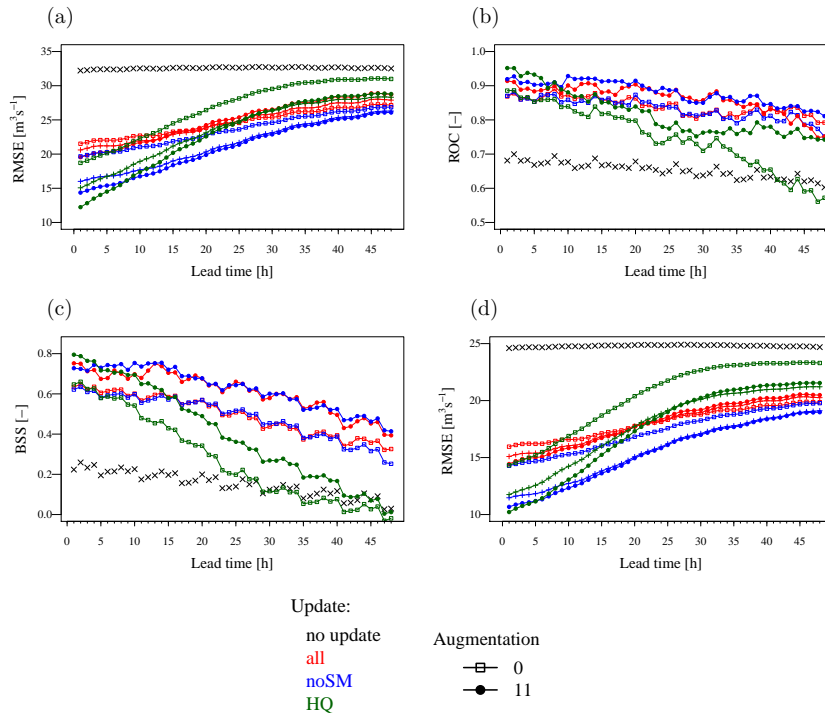


Figure 7. (a) Root-mean-square-error (RSME), (b) Relative operating characteristic (ROC), and (c) Brier skill score (BSS) at Tabreux (gauge 1) for different discharge observation vectors for which different model states are updated and with different lengths of the state augmentation vector (W) of past observations being assimilated. The results incorporate a set of 8 flood events shown in Table 1. Gauges 1, 3, 5, and 6 are assimilated. For BSS, the reference forecast is the sample climatology and only values larger than the 25th percentile of the whole sample are considered. (d) Same as (a) but the results are presented for Durbuy (gauge 2), a validation location which is not assimilated.

Asynchronous
filtering for
hydrological
forecasting

O. Rakovec et al.

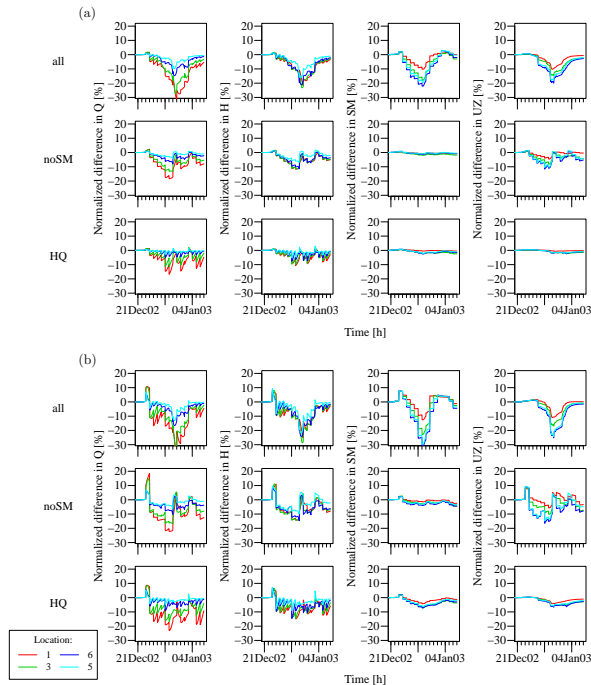


Figure 8. Scaled difference between the ensemble mean for the 3 partitioned update schemes and the control run without data assimilation at 4 gauging locations (shown by different colors) within the Upper Ourthe catchment using the AEnKF with (a) $W = 0$ and (b) $W = 11$. We dropped out the insensitive lower zone (LZ). Gauges 1, 3, 5, and 6 are assimilated. The results correspond to the same period as presented in Fig. 6.